Research Square

Preprints are preliminary reports that have not undergone peer review.
They should not be considered conclusive, used to inform clinical practice,
or referenced by the media as validated information.

Proteomic and functional insights into spinal neuroimmune maladaptation: dual-level modulation of mast cell-neural crosstalk by ultramicronized palmitoylethanolamide

Alessandra Toti

alessandra.toti@unifi.it

University of Florence

Maria Giovanna Cataldi

University of Florence

Laura Micheli

University of Florence

Elena Lucarini

University of Florence

Francesco Margiotta

University of Florence

Daniel Venturi

University of Florence

Gilda Aiello

Telematic University San Raffaele

Alfonsina D'Amato

University of Milan

Tommaso Mello

University of Florence

Carla Ghelardini

University of Florence

Lorenzo Di Cesare Mannelli

University of Florence

Research Article

Keywords:

Posted Date: October 23rd, 2026

DOI: https://doi.org/10.21203/rs.3.rs-10892364/v1

License: This work is licensed under a Creative Commons Attribution 4.0 International License.
Read Full License

Additional Declarations: No competing interests reported.

Proteomic and functional insights into spinal neuroimmune maladaptation: dual-level modulation of mast cell-neural crosstalk by ultramicronized palmitoylethanolamide

Alessandra Toti[1*^]; Maria Giovanna Cataldi[1*], Laura Micheli[1]; Elena Lucarini[1]; Francesco Margiotta[1,2]; Daniel Venturi[1,3]; Gilda Aiello[4], Alfonsina D'Amato[5]; Tommaso Mello[6]; Carla Ghelardini[1]; Lorenzo Di Cesare Mannelli[1].

[1]*Department of Neuroscience, Psychology, Drug Research and Child Health - NEUROFARBA - Pharmacology and Toxicology Section, University of Florence, Florence, Italy*

[2]*European Biomedical Research Institute of Salerno (EBRIS), Salerno, Italy*

[3]*Nuffield Department of Clinical Neuroscience, University of Oxford, Oxford, United Kingdom.*

[4]*Department of Human Science and Quality of Life Promotion, Telematic University San Raffaele, 00166 Rome*

[5]*Department of Pharmaceutical Sciences, University of Milan, Milan, Italy*

[6]*Department of Biomedical Clinical and Experimental Sciences "Mario Serio" - Clinical Gastroenterology Unit - University of Florence, Florence, Italy*

*These authors contributed equally

^Corresponding author: alessandra.toti@unifi.it; +39 0552758395; Viale G. Pieraccini 6, 50139, Firenze (FI), Italy.

Abstract

Repeated morphine administration drives spinal neuroimmune mechanisms contributing to analgesic tolerance and hyperalgesia. We investigated the contribution of mast cell-derived mediators to spinal neuroinflammation and the homeostatic effects of ultramicronized palmitoylethanolamide (PEA) using rat organotypic spinal cord slice cultures. Slices exposed to morphine were treated with conditioned medium from activated RBL-2H3 mast cells. Mast cell-derived conditioned medium induced a robust neuroinflammatory response, upregulating IL-6, IL-1β, CCL2, and PTX3 expression, and markedly enhancing the release of the pro-nociceptive neuropeptide CGRP. These alterations were accompanied by reduced neuronal marker expression and impaired astrocytic reactivity in the spinal dorsal horn. Notably, upstream mast cell pretreatment with PEA modified their secretory activity, blunting subsequent spinal inflammatory cascades. Quantitative proteomic analysis revealed that conditioned medium derived from PEA-treated RBL-2H3 cells extensively reshaped the spinal microenvironment, rescuing extracellular matrix components (such as collagen VI), downregulating neurodegenerative markers (including SIRT2 and BIN1), and inducing protective regulators like LGALS1. Downstream tissue-level application of ultramicronized PEA directly to the spinal slices replicated these beneficial actions, significantly attenuating inflammatory transcription and CGRP release while restoring neuronal and astrocytic homeostatic profiles. Collectively, these findings suggest that mast cell-derived factors promote spinal neuroimmune maladaptation, which is effectively countered by ultramicronized PEA via a dual-level mechanism acting on both the mast cell secretome and the spinal tissue interface. This integrated approach offers a promising translational strategy to preserve opioid efficacy and mitigate central sensitization.

Highlights

- Mast cell-derived mediators induce neuroinflammatory and pro-nociceptive signaling in spinal cord slices.
- PEA reprograms mast cell secretory activity and reduces inflammatory signaling.

- PEA preserves neuronal integrity and modulates astrocyte responses in mast cell-driven inflammation.

1. Introduction

Pain is a complex sensory and emotional experience associated with actual or potential tissue damage and involves coordinated activity across peripheral nociceptors, spinal dorsal horn circuits and supraspinal networks [1–3]. Beyond neuronal mechanisms, increasing evidence indicates that immune and glial cells contribute substantially to pain modulation through neuroimmune signaling processes that enhance neuronal excitability and promote central sensitization within the spinal cord [4].

Opioid analgesics remain the main pharmacological option for severe pain, acting predominantly through μ-opioid receptor signaling to inhibit nociceptive transmission at spinal and supraspinal levels [5]. However, repeated opioid exposure frequently leads to analgesic tolerance and opioid-induced hyperalgesia, limiting long-term therapeutic efficacy [6]. In addition to classical receptor desensitization mechanisms, opioid tolerance is increasingly recognized as a neuroimmune phenomenon. Morphine activates glial cells and inflammatory signaling pathways within the spinal cord, creating a permissive environment that reduces analgesic responsiveness and promotes maladaptive plasticity [4,7,8].

Among the immune components involved in neuroimmune regulation, mast cells are emerging as important modulators of nervous system function. Located at neurovascular and meningeal interfaces, mast cells release cytokines, chemokines and proteases capable of influencing neuronal excitability, glial activation and extracellular matrix organization [9,10]. Evidence suggests that mast cell-derived mediators contribute to spinal neuroinflammation and pain amplification, highlighting a bidirectional crosstalk between mast cells and neural tissue that may also participate in opioid maladaptation [11,12].

N-palmitoylethanolamine (PEA) is an endogenous lipid mediator with anti-inflammatory and anti-

hyperalgesic properties, acting primarily as a homeostatic regulator of non-neuronal cell activity, including mast cells and glia [13]. Due to its highly lipophilic nature and poor water solubility, native PEA exhibits low dissolution rates and limited gastrointestinal absorption. To overcome these pharmacokinetic limitations, technological modification through jet milling is required to reduce particle size, thereby increasing its surface area and oral bioavailability [14,15]. Consequently, ultramicronized PEA displays improved bioavailability and tissue distribution compared with native PEA, reaching central nervous system structures such as the spinal cord [16]. Preclinical studies have shown that ultramicronized PEA prolongs morphine analgesia and delays tolerance development during repeated opioid administration [17]. Moreover, recent evidence indicates that it can regulate mast cell degranulation and modify mast cell-astrocyte communication, supporting the hypothesis that its beneficial actions involve modulation of mast cell-nervous tissue interactions [18,19].

To investigate neuroimmune mechanisms in a multicellular context that preserves tissue architecture and cellular interactions, organotypic spinal cord slice cultures represent a valuable ex vivo model bridging simplified *in vitro* systems and *in vivo* conditions [20,21]. These preparations maintain neuron-glia communication and allow controlled manipulation of inflammatory and pharmacological stimuli within intact spinal circuitry.

In the present study, we investigated whether ultramicronized PEA modulates neuroinflammatory and pro-nociceptive signaling induced by mast cell mediators and morphine within organotypic spinal cord slices, with particular focus on the functional and molecular consequences of mast cell-nervous tissue crosstalk.

2. Material and methods

2.1 *Study approval*

All animal manipulations were carried out according to the Directive 2010/63/EU of the European parliament and of the European Union council (22 September 2010) on the protection of animals used

for scientific purposes and in compliance with the International Association for the Study of Pain (IASP) guidelines.

The ethical policy of the University of Florence complies with the Guide for the Care and Use of Laboratory Animals of the US National Institutes of Health (NIH Publication No. 85-23, revised 1996; University of Florence assurance number: A5278-01).

Formal approval to conduct the experiments described was obtained from the Italian Ministry of Health (No. 17.E9C.N.NOV) and the Animal Subjects Review Board of the University of Florence. Experiments involving animals have been reported according to ARRIVE guidelines [22]. All efforts were made to minimize animal suffering and to reduce the number of animals used.

2.2 *Preparation of rat organotypic spinal cord slice cultures*

Organotypic spinal cord slices were prepared according to Toti et al. (2025)[23]. Briefly, spinal cords were removed from 4- to 6-day old male and female Sprague Dawley rat pups (Envigo, Varese, Italy) and exposed. Transverse slices (420 μm) were prepared using a McIlwain tissue chopper and transferred onto 30-mm diameter semiporous membranes inserts (Millicell-CM PICM03050; Millipore, Italy), which were placed in six well tissue culture plates containing 1.2 mL medium per well. The culture medium consisted of 50% Minimal Essential Medium (MEM), 25% Donor Horse Serum Heat-Inactivated, 25% Hanks' balanced salt solution (HBSS), 5 mg/mL glucose, 2 mM L-glutamine, 3.75 mg/mL amphotericin B and 1% penicillin (100 U/mL) and streptomycin (100 μg/mL). Slices were maintained at 37 °C in an incubator in an atmosphere of humidified air and 5% CO_2 for 14 days. During *in vitro* maturation, the slices reduced their initial thickness while maintaining their original structural integrity [23]. Prior to experiments, all the slices were screened for viability by phase-contrast microscopy analysis; slices displaying signs of neurodegeneration were discarded from the study (exclusion criteria).

2.3 *Organotypic spinal cord cultures treatments*

Rat basophilic leukemia (RBL-2H3) mast cell line was used. RBL-2H3 cells were pre-sensitized with anti-dinitrophenyl (DNP)-IgE (50 ng/mL) for 18 h in the absence (untreated) or presence of ultramicronized palmitoylethanolamide (PEA, 100 μM). The following day, cells were washed to remove PEA and subsequently stimulated with dinitrophenyl-bovine serum albumin (DNP-BSA; 625 ng/mL) for 24 h to induce degranulation. At the end of stimulation, culture media were collected and used as conditioned media (c.m.).

In parallel, organotypic spinal cord slices were exposed to morphine (30 μM) for 48 h. Following morphine treatment, slices were incubated for 6 h with c.m. derived from untreated and PEA-treated RBL-2H3 cells. Prior to application to spinal cord slices, the c.m. was diluted 1:2 with culture medium (Supplementary Fig. 1A).

For experiments assessing the direct effects of PEA on spinal cord tissue, slices were incubated with c.m. from untreated RBL-2H3 cells either alone or in combination with PEA (50 nM) for 6 h (Supplementary Fig. 1B).

2.4 *RNA isolation, Reverse Transcription and RT-PCR*

Total RNA was isolated from rat organotypic spinal cord slices using TRI Reagent (Merck, Milan, Italy). 500 ng of RNA was retrotranscribed using PrimeScript™ RT reagent Kit with gDNA eraser. RT-PCR was performed using SsoAdvanced Universal SYBR⁻ Green Supermix following the thermal profile suggested by the kit. The primer used are reported in Table 1 (Invitrogen, Monza, Italy).

rCCL2	Fw: 5'-TCTTCCTCCACCACTATGCAGGTCTC-3' Rv: 5'-TCTTTGGGACACCTGCTGCTGGTG-3'
rPTX3	Fw: 5'-AAACTTCGCCTCTCCAGCAATGCATC-3' Rv: 5'-TGAACAGCTTGTCCCACTCCGAGTG-3'

rGFAP	Fw: 5'-CTGACACACGTTGTGTTCAAGCAGCC-3' Rv: 5'-CTGAAGGTTAGCAGAGTTGACAAGGG-3'
rSCL1A3	Fw: 5'-CAGTCATCGTCGGCCTCCTCATTC-3' Rv: 5'-CTGGTGATGCGTTTGTCCACACCATTG-3'

Table 1. List of forward and reverse primers used for RT-PCR

The following validated primers were purchased from Bio-Rad: rIL-6 (qRnoCID0004680), rIL-1B (qRnoCID0004680), rScl1a2 (qRnoCED0005967) and rβ2microglobulin as housekeeping (qRnoCED0056999). The differential expression of the transcripts is normalized on the housekeeping gene.

2.5 *Biochemical analysis*

At the end of the treatments, the culture medium was collected for biochemical analysis. Concentrations of calcitonin gene-related peptide (CGRP) were assessed by enzyme-linked immunosorbent assay (ELISA) (Biomatik, Ontario, Canada. cod. EKF58049), according to the manufacturer's instructions. Levels were normalized to cell protein concentrations quantified by BCA assay (Merck, Milan, Italy). Control conditions in the absence of treatment were arbitrarily set as 100% and all results are expressed as percentage in comparison with the control.

2.6 *Immunofluorescence staining in free-floating*

Organotypic spinal cord slice cultures were fixed and processed for immunofluorescence as previously described by Toti et al. (2025)[23] with minor modifications. After fixation with cold 4% paraformaldehyde at 4 °C overnight, slices were blocked in TBS containing 0.3% Triton X-100 and 10% normal goat serum. Slices were incubated overnight at 4 °C with the following primary antibodies: chicken anti-GFAP (1:1000; PA1-10004, Life Technologies, Monza, Italy), rabbit anti-NeuN (1:200; GTX132974, Genetex, TX, USA), and rabbit anti-Iba1 (1:200; Wako Chemicals USA, VA, USA). This

was followed by incubation with Alexa Fluor 647 goat anti-chicken secondary antibody (1:1000; Life Technologies, Monza, Italy) and Alexa Fluor 568 goat anti-rabbit secondary antibody (1:1000; Life Technologies, Monza, Italy). Nuclei were counterstained with DAPI, and slices were mounted using Fluoromount prior to imaging. Images were acquired using a motorized Leica DM6000 B fluorescence microscope. Image analysis was performed using ImageJ software (NIH, Bethesda, MD, USA). GFAP and NeuN fluorescence intensity was quantified from two fields per slice (8 or 15 slices total) using a 20× objective, while $NeuN^+$ cell counts were obtained from four fields per slice (8 or 15 slices total) using a 40× objective.

2.7 *Secretome, proteome and bioinformatic analysis*

Two complementary proteomic analyses were performed. Secretome analysis was carried out on conditioned media collected from untreated and PEA-treated RBL-2H3 cells after 24 h of DNP-BSA stimulation. In parallel, proteomic analysis was performed on organotypic spinal cord slices treated or not with morphine and exposed to RBL-2H3 c.m. for 6 h; the c.m. was then replaced with fresh medium, and the slices were collected the following day. Each lyophilized medium and each slice were homogenized and tryptic digested as in D'Amato et al. (2020)[24]. The peptides were analyzed using a Dionex Ultimate 3000 nano-LC system (Sunnyvale CA, USA) connected to Orbitrap Fusion™ Tribrid™ Mass Spectrometer (Thermo Scientific, Bremen, Germany) equipped with a nano-electrospray ion source (nESI). Mobile phases were the following: 0.1% formic acid (FA) in water (solvent A), 0.1% FA in acetonitrile (solvent B). The elution gradient consisted of 4-28% B for 90 min and then 28–40% for 10 min, followed by 95% for the next 6 min to rinse the column [25]. The instrumental raw files were processed by MaxQuant software v1.6.6.0 [26] set on Uniprot_Rat database against the Andromeda search engine [24]. The quantification of peptides and related proteins for each sample in biological replicate and technical triplicates was based on the LFQ intensities. The interpretation and visualization of results obtained from MaxQuant software were performed by a two-

sample t-test using Perseus (v1.6.1.3, Max Planck Institute of Biochemistry, Germany). Statistical parameters ($p < 0.05$; $q < 0.05$, q= FDR adjusted p-value) were set to identify the differentially expressed proteins between samples (log2 ratio). Variability of biological replicates were measured using the scatter plot with Pearson correlation coefficient values of the LFQ intensities. The network protein analysis related to significantly altered proteins was carried out by Ingenuity Pathways Analysis (IPA) (last release; Qiagen) based on Gene Ontology database [25].

2.8 *Cytotoxicity assay*

For toxicity evaluation, the release of lactate dehydrogenase (LDH) into the culture media was determined using a Cytotoxicity Detection Kit (Roche 11644793001, Roche Diagnostics GmbH Roche Applied Science Mannheim, Germany) according to the manufacturer's protocol. Each value corresponds to a well, with five slices per transwell, and a total of six samples (n=6) were analyzed. LDH levels were normalized to cell protein concentrations, quantified by bicinchoninic acid (BCA) assay (Merck, Milan, Italy). Control conditions in the absence of treatment were arbitrarily set as 100%, and all results are expressed as percentage in comparison with the control.

2.9 *Statistics*

Results were expressed as a mean ± S.E.M., and statical analysis was performed using ONE-way or TWO-way ANOVA. Bonferroni's post hoc test was applied for multiple comparisons. P values less than 0.05 were considered statistically significant. Data were analyzed using "Origin® 9.1" software.

3. Results

3.1 Ultramicronized PEA modulates morphine-induced neuroinflammatory gene expression via mast cell mediators in organotypic spinal cord cultures

Our previous work showed that ultramicronized palmitoylethanolamide (PEA; 100 μM, 18 h) significantly modulates DNP-BSA-induced degranulation of the rat basophilic leukemia mast cell line RBL-2H3 (Toti et al., 2023). Secretome analysis further demonstrated that PEA reduces the release of several degranulation-associated and inflammatory mediators, including β-hexosaminidase, mast cell protease 2, GM2 activator protein, and the chemokine C-C motif chemokine ligand 2 (CCL2) (Supplementary Fig. 2 and Supplementary Tab. 1).

To investigate the functional consequences of mast cell signaling in a more integrated CNS context, particularly under opioid exposure, we employed rat organotypic spinal cord slice cultures, an *ex vivo* model that preserves cellular heterogeneity and neuroimmune interactions.

Preliminary experiments identified 30 μM morphine as the highest concentration that did not compromise slice viability (Supplementary Fig. 3A).

Notably, while conditioned media (c.m.) from untreated RBL-2H3 cells induced significant cellular toxicity, indicated by LDH levels (Supplementary Fig. 3B), this effect was completely absent when c.m. was derived from mast cells treated with PEA. Therefore, to ensure uniform and non-toxic conditions across all experimental groups, all c.m. were diluted 1:2 prior to spinal cord slice application (Supplementary Fig. 3C).

Slices were exposed to morphine (30 μM) for 48 h, followed by a 6-h incubation with c.m. derived from either untreated or PEA-treated RBL-2H3 cells (100 μM PEA, 18 h). Gene expression of neuroinflammatory and glutamatergic markers was then assessed by RT-PCR.

In control slices treated with c.m. from untreated RBL-2H3 cells, the expression of the pro-inflammatory mediators interleukin-6 (IL-6), interleukin-1β (IL-1β), CCL2, and pentraxin-3 (PTX3) was significantly increased compared with control slices (Fig. 1A). A non-significant trend toward

increased expression of the glial glutamate transporter excitatory amino acid transporter 1 (EAAT1) was also observed, whereas glial fibrillary acidic protein (GFAP) and excitatory amino acid transporter 2 (EAAT2) expression remained unchanged (Fig. 1B).

Conditioned medium derived from PEA-pretreated RBL-2H3 cells significantly reduced the expression of all the above-mentioned pro-inflammatory genes. EAAT1 expression also decreased under this condition, reflecting an attenuation of reactive glial responses (Fig. 1A-B).

A comparable pattern was observed in morphine-treated slices. Exposure to c.m. from untreated RBL-2H3 cells increased IL-6, IL-1β, PTX3, and CCL2 expression compared with control, whereas c.m. from PEA-pretreated cells attenuated these responses (Fig. 1A). In contrast, GFAP and EAAT2 expression showed a different profile: morphine-treated slices incubated with c.m. from untreated RBL-2H3 cells displayed reduced expression of both genes compared to CTR, while treatment with c.m. from PEA-pretreated cells significantly increased their expression (Fig. 1B).

Finally, a comparison between control slices and morphine-treated slices, both incubated with untreated RBL-2H3-derived c.m., revealed a markedly higher IL-1β expression in the morphine group, suggesting an additive or synergistic interaction between morphine exposure and mast cell-derived inflammatory signals.

Overall, these findings indicate that mast cell-derived soluble mediators strongly influence neuroinflammatory and glutamatergic gene expression in spinal cord tissue. Moreover, PEA pretreatment appears to reprogram mast cell signaling, reducing pro-inflammatory responses while promoting astrocyte-associated homeostatic pathways, particularly in the context of morphine exposure.

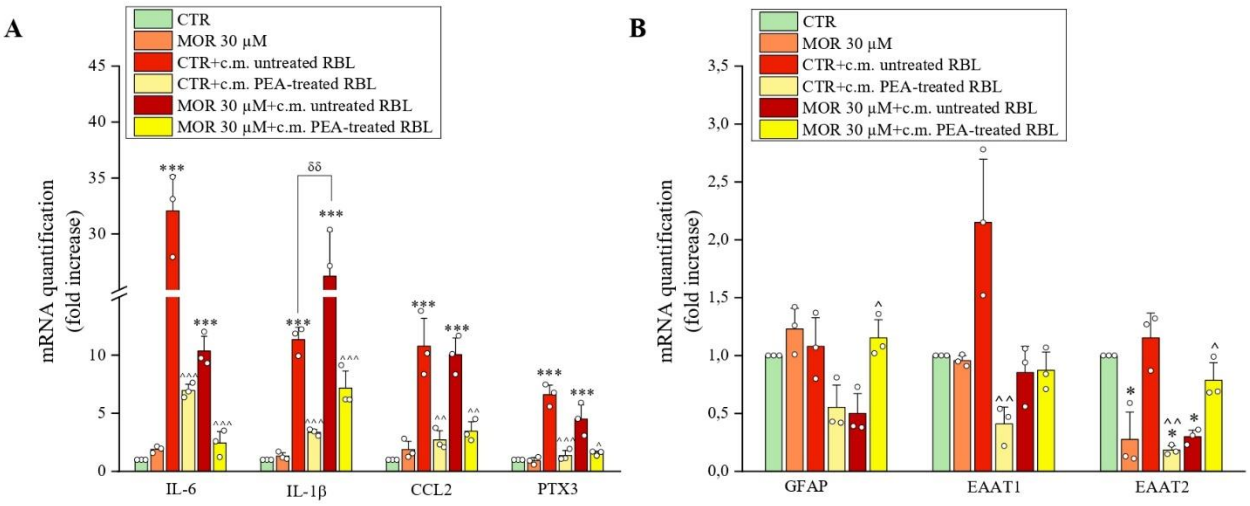


Figure 1. Ultramicronized PEA modulates neuroinflammatory and glutamatergic gene expression in organotypic spinal cord cultures. *(A-B) Slices were treated with morphine (MOR, 30 µM) for 48 h and subsequently incubated for 6 h with c.m. derived from RBL-2H3 cells stimulated with DNP-BSA (625 ng/mL) and either untreated or pretreated with ultramicronized PEA (100 µM, 18 h). Data are presented as mean ± S.E.M. of three independent experiments. *P < 0.05, ***P < 0.001 vs CTR slices; ^P < 0.05, ^^P < 0.01, ^^^P < 0.001 vs slices + c.m. untreated RBL; $^{\delta\delta}$P < 0.01 MOR + c.m. untreated RBL vs CTR + c.m. untreated RBL.*

3.2 Ultramicronized PEA modulates mast cell-mediated regulation of CGRP release in morphine-treated spinal cord slices

In order to assess pro-nociceptive signaling, calcitonin gene-related peptide (CGRP) release into the culture medium was measured by ELISA kit, under the same experimental conditions described above.Morphine exposure (30 µM, 48 h) significantly reduced CGRP release from spinal cord slices compared with control conditions (Fig. 2). In control slices, incubation with c.m. from untreated RBL-2H3 cells significantly increased CGRP levels, indicating that mast cell-derived soluble mediators stimulate CGRP release in spinal tissue.

This effect was markedly attenuated by PEA-treatment of RBL-2H3 cells, suggesting that PEA down-modulates mast cell secretory activity and reduces the ability of mast cell mediators to promote CGRP release.

In morphine-treated slices, incubation with c.m. from untreated RBL-2H3 cells did not significantly

modify CGRP levels compared with morphine treatment alone. In contrast, exposure to c.m. derived from PEA-treated RBL-2H3 cells produced a further reduction in CGRP release.

Overall, these findings indicate that mast cell-derived soluble factors regulate CGRP release in spinal cord tissue and that PEA pretreatment of mast cells modifies this signaling, limiting CGRP release under basal conditions and further enhancing the morphine-induced reduction of CGRP levels.

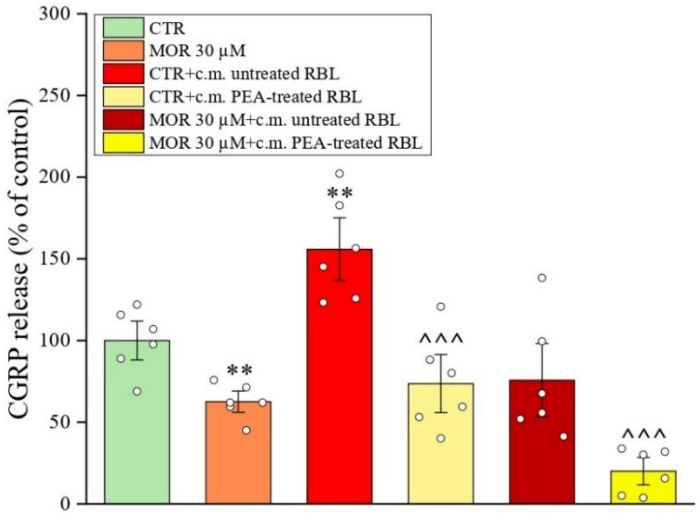


Figure 2. Mast cell-derived mediators and PEA regulate CGRP release in morphine-treated spinal cord slices. *CGRP release from rat organotypic spinal cord slice cultures exposed to mast cell-conditioned media under basal conditions or following morphine treatment. Slices were treated with morphine (30 µM) for 48 h and subsequently incubated for 6 h with c.m. derived from RBL-2H3 cells stimulated with DNP-BSA (625 ng/mL) and either untreated or pretreated with ultramicronized PEA (100 µM, 18 h). After treatments, the culture medium was replaced with fresh serum-free medium, and CGRP levels in the supernatant were measured following an 18 h collection period. CGRP release is expressed as percentage of control slices, which were arbitrarily set to 100%. Data represent the mean ± S.E.M. of three independent experiments in duplicates (n = 6). **P<0.01 vs CTR slices; ^^^ P< 0.001 vs slices +c.m. untreated RBL.*

3.3 Conditioned medium from ultramicronized PEA-treated mast cells enhances neuronal survival and modulates astrocyte activation

To elucidate the underlying mechanisms, the response of neurons, astrocytes, and microglia in the spinal cord slices was further investigated.

Neuronal integrity was evaluated by quantifying the number and fluorescence intensity of neuronal nuclei-positive cells ($NeuN^+$), a selective marker for mature neurons. As shown in Figure 3A, while morphine treatment alone had no effect, exposing morphine-treated spinal cord slices to c.m. from untreated RBL-2H3 cells significantly reduced the number of $NeuN^+$ cells compared with control slices. In contrast, incubation with c.m. derived from PEA-pretreated RBL-2H3 cells markedly rescued this effect, increasing $NeuN^+$ cell count in morphine-treated slices compared with those exposed to untreated c.m. Similarly, exposure of control slices to PEA-treated c.m. resulted in a higher number of $NeuN^+$ cells compared with slices exposed to c.m. from untreated cells. Notably, $NeuN^+$ cell numbers in morphine-treated slices exposed to PEA-c.m. exceeded those observed in control slices treated with the same medium. This indicates that the neuroprotective effect of ultramicronized PEA is particularly pronounced to counterbalance the marked neurotoxicity induced by co-exposure to morphine and untreated RBL-2H3 cell c.m. Analysis of NeuN fluorescence intensity (Fig. 3B) revealed no significant differences among most experimental groups; however, a significant increase was detected in control slices treated with PEA-c.m. compared with untreated control slices. Representative NeuN immunofluorescence images are shown in Figure 3C.

Astrocyte activation was assessed by measuring GFAP immunoreactivity. As shown in Figure 3D, control slices incubated with c.m. from untreated RBL-2H3 cells showed reduced GFAP fluorescence intensity which was rescued by c.m. from PEA-treated cells. Similarly, in morphine-treated slices, PEA-c.m. significantly increased GFAP expression compared with untreated c.m. Notably, morphine-treated slices exposed to c.m. derived from untreated RBL-2H3 cells displayed higher GFAP intensity than their respective controls, suggesting a prominent morphine-induced astrocytic response. Representative GFAP immunofluorescence images are shown in Figure 3E.

Microglial involvement was evaluated by measuring ionized calcium-binding adapter molecule 1 (IBA-1) immunoreactivity. Nevertheless, no significant differences were detected among the experimental groups (Supplementary Fig.4).

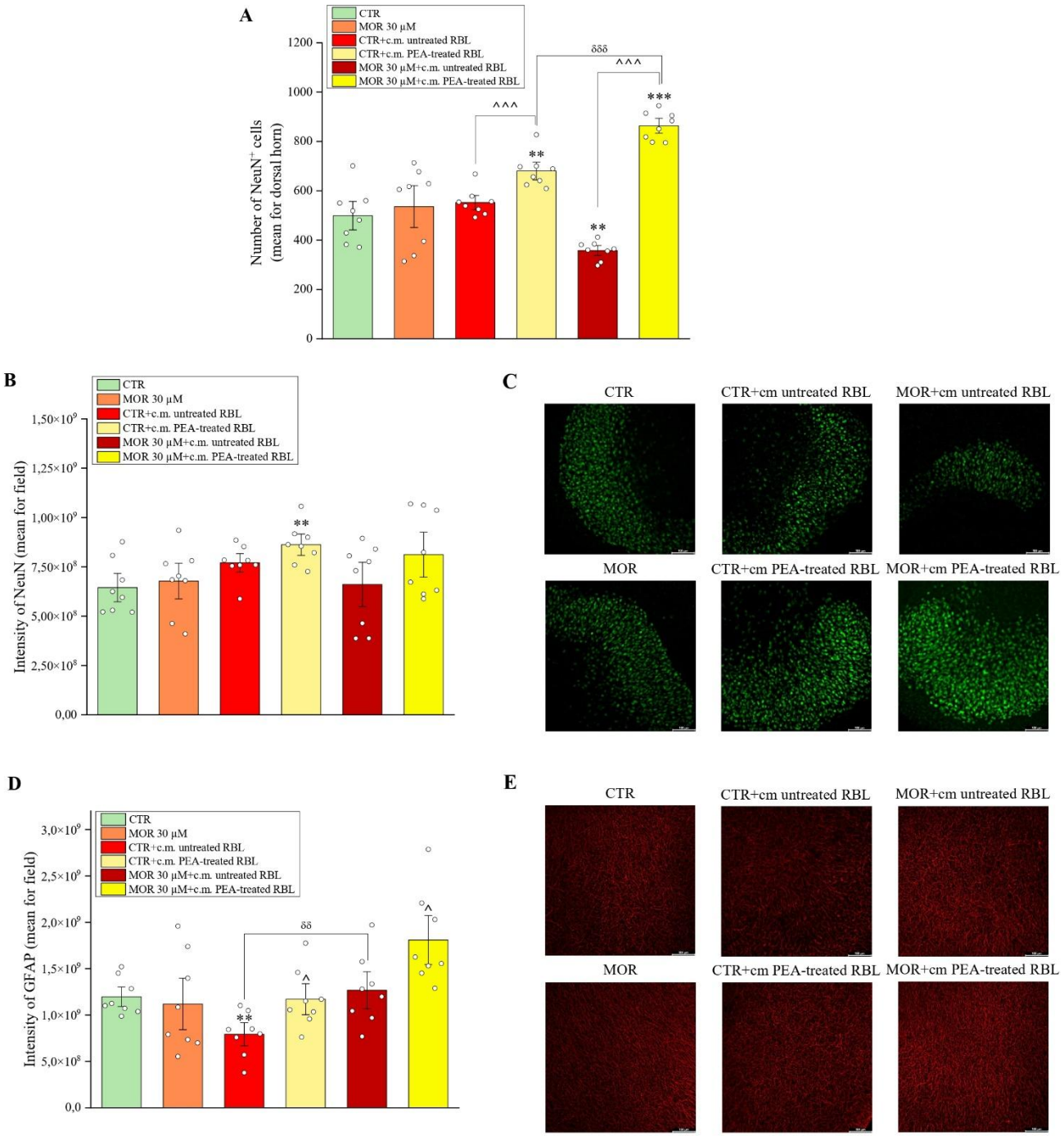


Figure 3. Effects of PEA-treated mast cell conditioned medium on neuronal viability and astrocyte activation.

Immunofluorescence analysis of neuronal viability and astrocytic activation in rat organotypic spinal cord slice

*cultures exposed to mast cell-conditioned media under basal conditions or following morphine treatment. Slices were treated with morphine (30 μM) for 48 h and subsequently incubated for 6 h with c.m. derived from RBL-2H3 mast cells stimulated with DNP-BSA (625 ng/mL) and either untreated or pretreated with ultramicronized PEA (100 μM, 18 h). After 6 h of c.m. exposure, slices were washed and maintained in fresh medium for an additional 18 h before immunofluorescence analysis. (A) Quantification of $NeuN^+$ cell number in the dorsal horn. (B) Quantification of NeuN fluorescence intensity in the dorsal horn. (C) Representative images of NeuN immunofluorescence. (D) Quantification of GFAP fluorescence intensity in the dorsal horn. (E) Representative images of GFAP immunofluorescence. Images were acquired using a 20× objective; scale bar = 100 μm. Data are expressed as mean ± S.E.M. of three independent experiments, with n = 8 slices per condition. **P<0.01 vs CTR slice. $^{\wedge}$P< 0.05; $^{\wedge\wedge\wedge}$P< 0.001 vs slices +c.m. untreated RBL. $^{\delta\delta}$P< 0.01; $^{\delta\delta\delta}$P< 0.001 MOR +c.m. PEA treated RBL vs CTR slices +c.m. PEA treated RBL.*

3.4 Proteomic profiling of spinal cord slices exposed to ultramicronized PEA-modulated mast cell conditioned medium

To further characterize the molecular changes associated with mast cell-mediated signaling and PEA modulation, a quantitative proteomic analysis of the organotypic spinal cord slices was performed under the same experimental conditions described above. Various comparisons were conducted to evaluate the respective effects of morphine, degranulated RBL-2H3 medium and PEA.

In slices exposed to morphine, 18 proteins were significantly modulated (15 up-regulated and 3 down-regulated) compared with untreated controls (Fig. 4A). Among the up-regulated proteins, we identified pathways involved in inflammatory signaling and cytoskeletal remodeling including profilin-1 (PFN1), dynein light chain roadblock-type 1 (DYLRB1), ADP-ribosylation factor 4 (ARF4), cold-inducible RNA-binding protein RBM3 (RBM3) and lamin-B2 (LMNB2). These findings indicate the activation of processes involved in cellular structural changes.

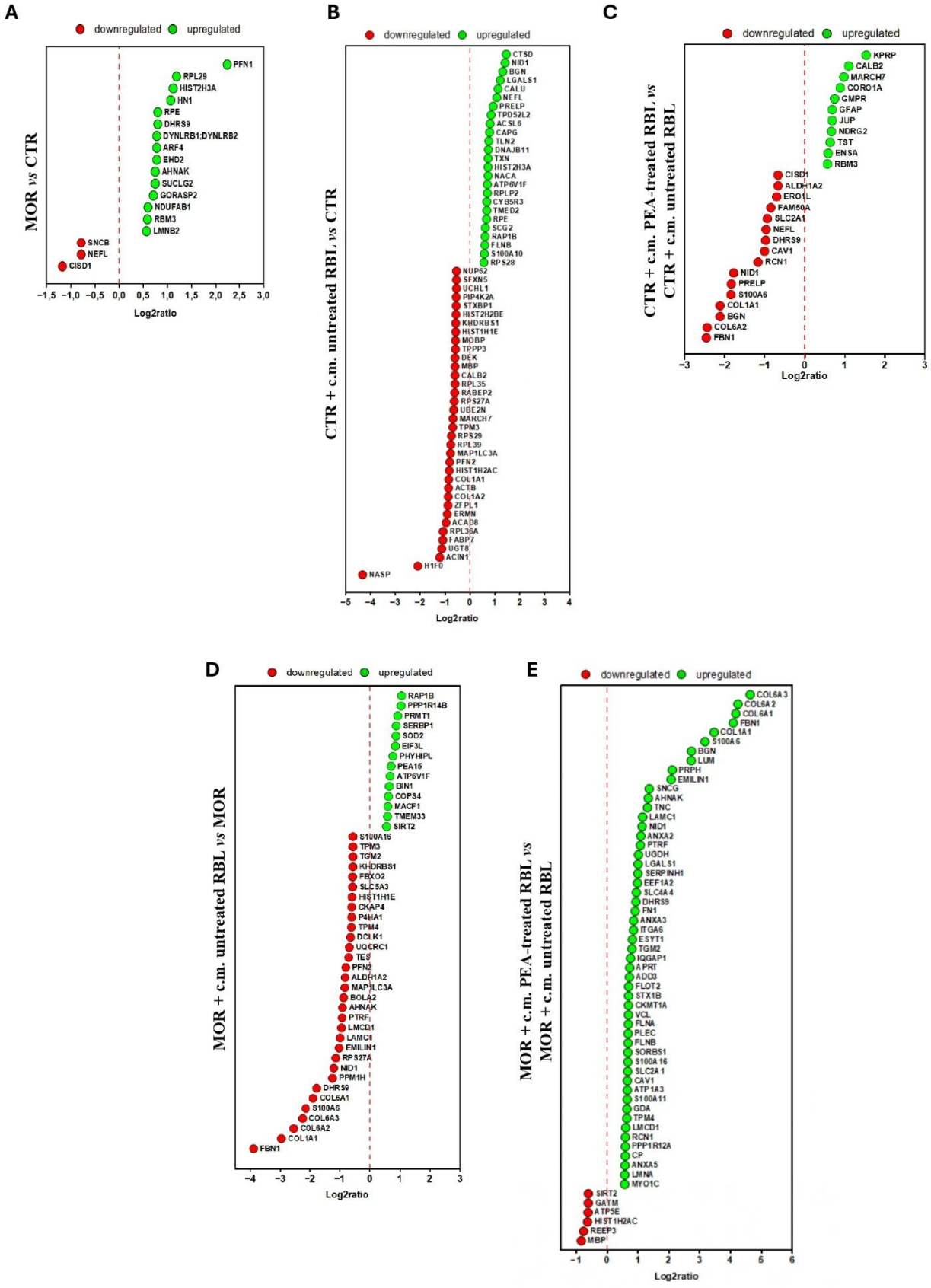
Exposure of control slices to c.m. from untreated RBL-2H3 cells changed the expression of 62 proteins, with 25 being upregulated and 37 downregulated proteins (Fig. 4B). Under this condition,

proteins associated with inflammatory activation and neuroimmune signaling, such as cathepsin-D (CTSD), biglycan (BGN), neurofilament light chain (NEFL), thioredoxin (TXN) and secretogranin-2 (SCG2) were upregulated, reflecting a strong pro-inflammatory shift. Conversely, numerous structural and myelin-associated proteins were downregulated, including collagen type I chains (COL1A1, COL1A2), UDP-glycosyltransferase-8 (UGT8), ermin (ERMN), myelin basic protein (MBP), myelin-associated oligodendrocyte basic protein (MOBP), ubiquitin C-terminal hydrolase L1 (UCHL1) and ubiquitin-conjugating enzyme E2N (UBE2N), pointing to weakened matrix stability and altered myelin organization.

In the third comparison, c.m. from PEA-pretreated RBL-2H3 cells induced a proteomic response involving 27 modulated proteins with 11 upregulated and 16 downregulated (Fig. 4C). This condition was characterized by increased expression of glial fibrillary acidic protein (GFAP) and N-myc downstream-regulated gene 2 (NDRG2), both associated with glial homeostasis. Conversely, we observed a downregulation of proteins typically linked to stress and pro-inflammatory pathways, such as ERO1-like protein alpha (ERO1L), glucose transporter GLUT1 (SLC2A1) and biglycan (BGN) indicating that PEA modulates mast cell-derived signaling, shifting it toward a less inflamed tissue environment.

Moreover, when morphine-treated slices were exposed to c.m from untreated RBL-2H3 cells, 46 proteins were significantly modulated (14 upregulated and 32 downregulated) (Fig. 4D). The combination of morphine with mast-cell mediators exacerbated changes in extracellular matrix (ECM) organization and innate immune signaling. Specifically, proteins such as Ras-related protein Rap1b (RAP1B), Myc box-dependent interacting protein-1 (BIN1) and sirtuin-2 (SIRT2) were increased. In contrast, several components involved in mitochondrial function, ECM stability, synaptic regulation and cytoskeletal integrity, including transglutaminase-2 (TGM2), F-box only protein-2 (FBXO2), Ubiquinol-Cytochrome C Reductase Core Protein 1 (UQCRC1), aldehyde dehydrogenase 1A2 (ALDH1A2), collagen I and VI chains (COL1A1, COL6A 1,2,3), AHNAK (AHNAK), calcyclin (S100A6) and fibrillin-1 (FBN1), were downregulated.

The final comparison, evaluating the effect of PEA-treated RBL-2H3 c.m. on morphine-exposed slices, revealed the most extensive proteomic modulation, with 53 upregulated and 6 downregulated proteins (Figure 4E). This condition recapitulated the main patterns identified in the earlier comparisons, namely the downregulation of inflammatory mediators and the concomitant upregulation of ECM components. Specifically, we observed a robust upregulation of collagen VI chains (COL6A 1,2,3), biglycan (BGN), lumican (LUM), fibronectin-1 (FN1) and tenascin-C (TNC), together with calcyclin (S100A6), AHNAK (AHNAK) and galectin-1 (LGALS1). Concurrently, proteins associated with cellular stress and degeneration, such as sirtuin-2 (SIRT2) and myelin basic protein (MBP), were reduced, suggesting that ultramicronized PEA attenuates neuroinflammatory damage and promotes tissue homeostasis.



407

408 ***Figure 4. Differential proteomic modulation of organotypic spinal cord slices across experimental***

409 ***conditions.***

Differentially expressed proteins identified by quantitative proteomic analysis in rat organotypic spinal cord slice cultures under the indicated experimental conditions. Each panel shows proteins significantly upregulated (green) or downregulated (red) in the specified comparison, based on a log2 ratio threshold of ≥ 0.56 or ≤ -0.56 with $p < 0.05$ (three biological replicates).

(A) Morphine-treated slices (MOR) versus untreated control slices (CTR).

(B) Control slices exposed to conditioned medium from untreated RBL-2H3 cells (CTR + c.m. untreated RBL) versus control slices.

(C) Control slices exposed to conditioned medium from ultramicronized PEA-treated RBL-2H3 cells (CTR + c.m. PEA-treated RBL) versus control slices exposed to conditioned medium from untreated RBL-2H3 cells.

(D) Morphine-treated slices exposed to conditioned medium from untreated RBL-2H3 cells (MOR + c.m. untreated RBL) versus morphine-treated slices.

(E) Morphine-treated slices exposed to conditioned medium from ultramicronized PEA-treated RBL-2H3 cells (MOR + c.m. PEA-treated RBL) versus morphine-treated slices exposed to conditioned medium from untreated RBL-2H3 cells.

3.5 Ultramicronized PEA directly suppresses pro-inflammatory gene expression in organotypic spinal cord slices under mast cell-induced inflammation

Building on the proteomic evidence indicating that PEA modulates inflammatory and tissue homeostasis-related pathways, we next investigated whether PEA could directly regulate neuroinflammatory responses in organotypic spinal cord slices. To model a mast cell-driven inflammatory environment, slices were exposed to c.m. diluted 1:2 from untreated RBL-2H3 cells. Specifically, the potential protective effects of PEA at the tissue level were evaluated by treating the slices for 6 h with untreated RBL-2H3 c.m., either alone or in combination with ultramicronized PEA (50 nM). This concentration was selected based on prior cytotoxicity assays to ensure tissue viability (Supplementary Fig. 5).

Quantitative RT-PCR analysis revealed that exposure to untreated RBL-2H3 c.m. markedly increased the expression of the pro-inflammatory genes IL-6, IL-1β, CCL2, and PTX3 compared with control slices, confirming the strong neuroinflammatory impact of mast cell-derived soluble mediators (Fig. 5). Treatment with PEA alone did not significantly affect the expression of these markers compared with controls, except for a modest reduction in IL-6 levels. In contrast, co-treatment with PEA significantly suppressed the RBL-2H3 c.m.-induced upregulation of the inflammatory genes (Fig. 5). Together, these results demonstrate that direct application of ultramicronized PEA to CNS tissue effectively counteracts mast cell-induced neuroinflammatory signaling, highlighting a dual modulatory role wherein PEA acts both at the level of mast cells and directly within the neural tissue.

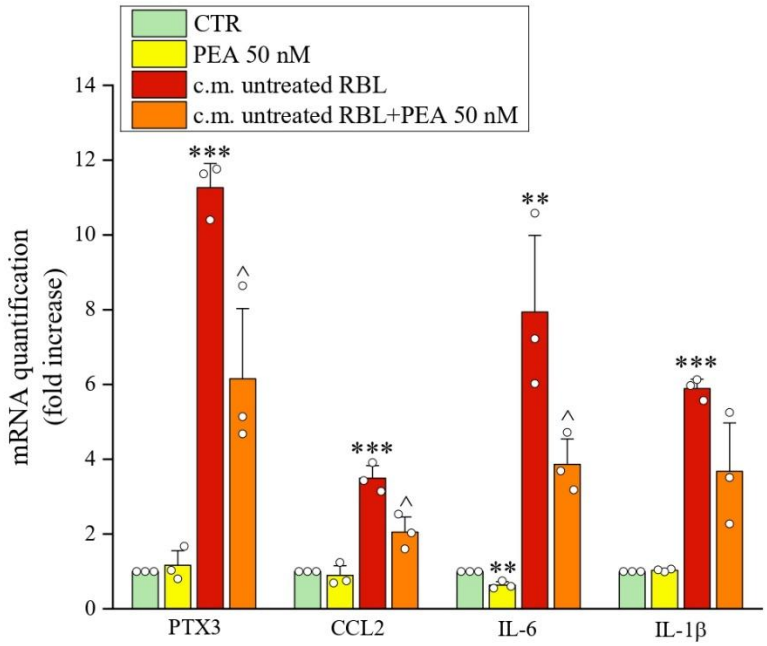


Figure 5. Effects of direct PEA treatment on inflammatory gene expression in organotypic spinal cord slices exposed to mast cell-conditioned medium.

Gene expression analysis by RT-PCR in rat organotypic spinal cord slice cultures exposed to c.m. from untreated RBL-2H3 cells in the absence or presence of ultramicronized PEA (50 nM). Slices were treated with RBL-2H3 c.m. alone or in combination with PEA for 6 h. mRNA levels of pro-inflammatory markers were quantified and normalized to housekeeping genes. mRNA values (gene expression) are reported as fold change relative to control slices, which were arbitrarily set to 1. Data represent the mean ± S.E.M. of three

*independent experiments. **P < 0.01, ***P < 0.001 vs CTR; ^P < 0.05 vs slices treated with c.m. from untreated RBL-2H3.*

3.6 Ultramicronized PEA modulates mast cell-mediated pro-nociceptive signaling in organotypic spinal cord slices

To further investigate the pro-nociceptive effects of mast cell-derived mediators and the modulatory role of PEA, CGRP release was quantified under the same experimental conditions. As shown in Figure 6, treatment of organotypic spinal cord slices with PEA alone (50 nM) did not significantly affect CGRP release compared with control slices.

In contrast, exposure to c.m. from untreated RBL-2H3 cells resulted in a marked increase in CGRP release, reaching approximately 60% above control levels. Co-treatment with PEA significantly counteracted this increase, bringing CGRP release back to baseline levels.

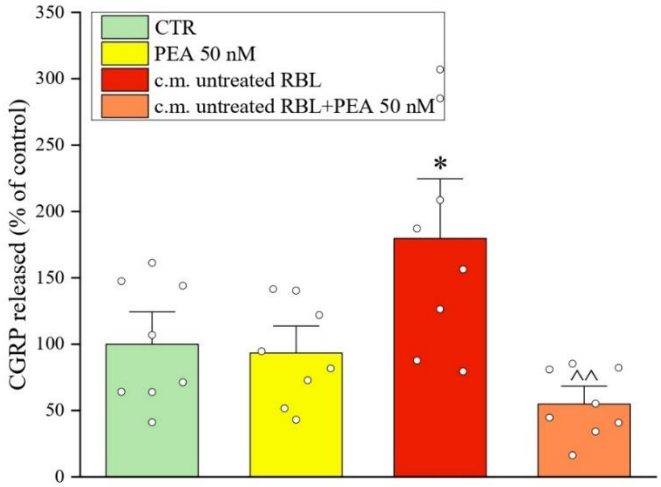
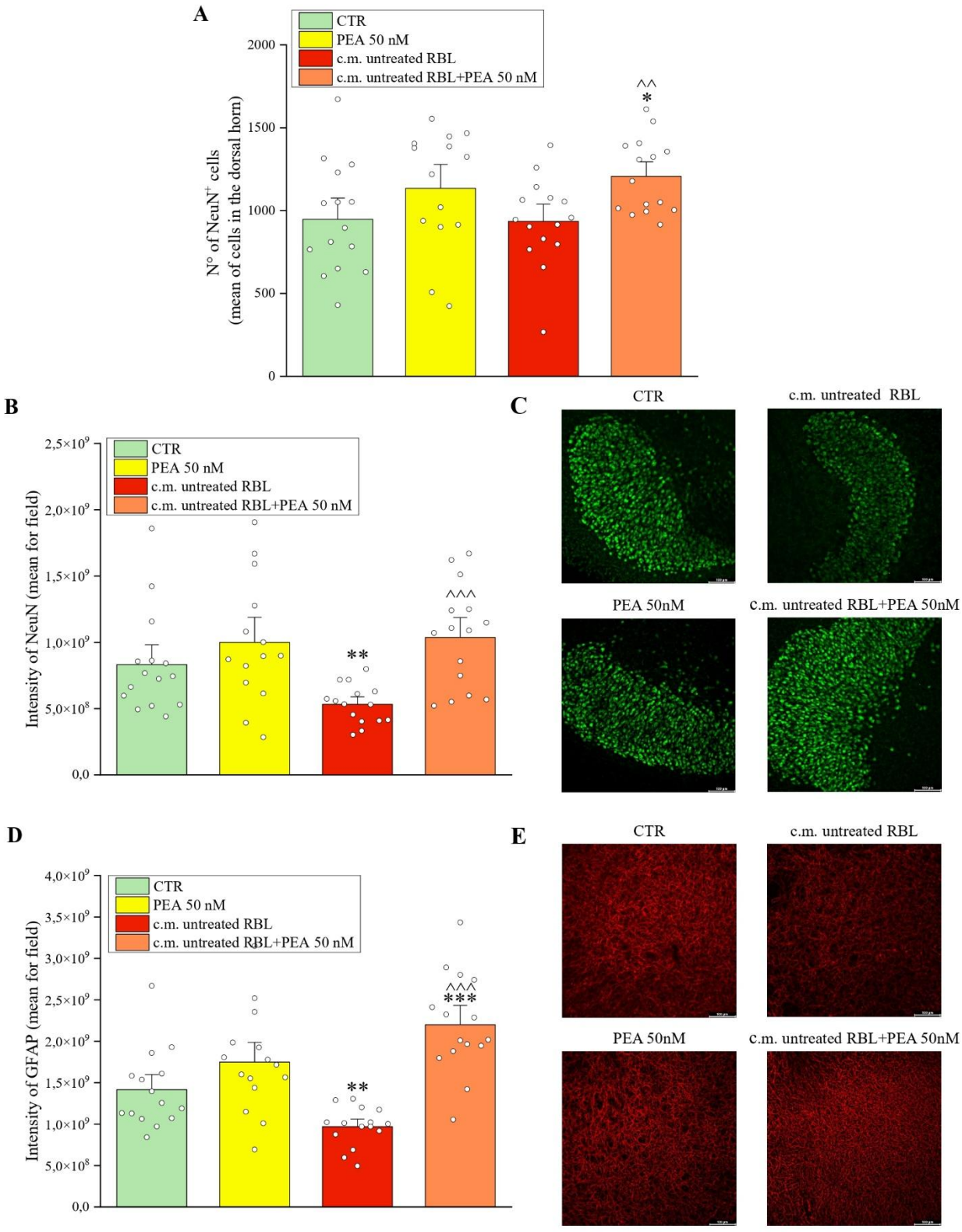


Figure 6. Effects of PEA on CGRP release induced by mast cell-conditioned medium in spinal cord slices. *Quantification of CGRP release from rat organotypic spinal cord slice cultures exposed to c.m. from untreated RBL-2H3 cells in the absence or presence of ultramicronized PEA (50 nM). Slices were treated with RBL-2H3 c.m. alone or in combination with PEA for 6 h. CGRP levels in the culture medium are expressed as mean ± S.E.M. (n = 8). *P < 0.05 vs CTR; ^^P < 0.01 vs slices treated with c.m. untreated RBL.*

3.7 Ultramicronized PEA preserves neuronal integrity and modulates astrocyte reactivity in spinal cord slices exposed to conditioned medium from stimulated mast cells

To evaluate the effects of mast cell-induced inflammation and the modulatory action of PEA on neuronal markers, NeuN immunofluorescence was analyzed in organotypic spinal cord slices. Representative images (Figure 7C) revealed evident morphological differences in the dorsal horn region across experimental conditions. In particular, slices co-exposed to untreated RBL-2H3 c.m. and PEA displayed a more robust dorsal horn area compared with slices exposed to untreated c.m. alone, suggesting a role for PEA in preserving tissue architecture. This finding is consistent with the observation from $NeuN^+$ cell quantification. As reported in figure 7A, while the untreated RBL-2H3 c.m. alone did not alter neuronal counts, a statistically significant increase in $NeuN^+$ cell number was detected in slices co-exposed to PEA and untreated RBL-2H3 c.m. compared with both control slices and slices exposed to untreated c.m. alone. This overall trend was further corroborated by fluorescence intensity measurements from an independent experimental set. As shown in Figure 7B, exposure to c.m. from untreated RBL-2H3 cells induced a robust neurotoxic effect, significantly decreasing NeuN fluorescence intensity relative to control slices. Crucially, direct co-treatment with 50 nM PEA completely prevented this loss, successfully maintaining NeuN fluorescence intensity at baseline levels.

Astrocyte reactivity was evaluated by quantifying GFAP immunofluorescence in the dorsal horn. As shown in Figures 7D and 7E, exposure to untreated RBL-2H3 c.m. was associated with a significant reduction in GFAP fluorescence intensity. In contrast, slices co-treated with PEA and untreated RBL-2H3 c.m. exhibited a marked increase in GFAP signal compared with the untreated c.m. condition, effectively preventing this loss.



499

500 ***Figure 7. Neuronal and astrocytic marker modulation in organotypic spinal cord slices exposed to mast cell-***

501 ***conditioned medium and PEA.***

502 *Immunofluorescence analysis of the neuronal marker (NeuN) and astrocytic marker (GFAP) in rat organotypic*

503 *spinal cord slice cultures exposed to mast cell c.m. in the absence or presence of ultramicronized PEA (50 nM).*

*Slices were treated with c.m. from untreated RBL-2H3 cells alone or in combination with PEA for 6 hours. Slices were then washed and maintained in fresh medium for an additional 18 h before immunofluorescence analysis. (A) Quantification of NeuN⁺ cell number in the dorsal horn. (B) Quantification of NeuN fluorescence intensity in the dorsal horn (C) Representative images of NeuN immunofluorescence. (D) Quantification of GFAP fluorescence intensity in the dorsal horn. (E) Representative images of GFAP immunofluorescence. Images were acquired using a 20× objective; scale bar = 100 µm. Data are expressed as mean ± S.E.M. of three independent experiments, with n = 14 or 15 slices per condition. **P < 0.01 vs CTR; ^^P < 0.01, ^^^P < 0.001 vs slices exposed to c.m. untreated RBL.*

4. Discussion

The present study demonstrates that mast cell-derived mediators critically shape the neuroimmune environment of the spinal cord both in basal conditions and morphine exposure. Moreover, it shows that ultramicronized PEA effectively orchestrates a dual-level modulation of this crosstalk within a complex multicellular context, acting both upstream on mast cell secretory phenotypes and downstream directly within neural tissue. Exposure of organotypic spinal cord slices to conditioned medium derived from degranulated RBL-2H3 cells was sufficient to trigger a coordinated neuroinflammatory response. The findings align with previous studies indicating mast cells as regulators of the spinal neuroimmune milieu through the release of soluble mediators capable of shaping neuronal-glial communication and tissue homeostasis [9,27–29]. Accordingly, the robust upregulation of IL-6, IL-1β, CCL2 and PTX3 is consistent with established evidence that mast cell-derived soluble factors activate innate immune signaling and promote central sensitization. In the dorsal horn, cytokines like IL-1β and IL-6 directly enhance excitatory synaptic transmission, while CCL2/CCR2 signaling drives microglia activation and amplifies persistent pain loops [30–32].

At a functional level, mast cell-derived factors significantly stimulated the release of CGRP from spinal cord slices. Beyond its classical role in nociceptive neurotransmission, CGRP serves as a potent

530 neuroimmune amplifier by activating intracellular cascades in spinal glia, thereby sustaining chronic
531 neuroinflammatory states and persistent pain [33–36]. The increase in CGRP observed in our model
532 therefore supports the idea that mast cell-derived mediators are sufficient to engage pro-nociceptive
533 neuroimmune pathways in intact spinal tissue.
534 Notably, morphine reduced CGRP release, consistent with its canonical analgesic action. In
535 morphine-exposed slices, mast cell-conditioned medium did not increase CGRP release, suggesting
536 that opioid signaling modifies the spinal response to mast cell-derived mediators. Conditioned
537 medium from PEA-treated mast cells further reduced CGRP release, indicating that modulation of
538 the mast cell secretome can restrain pro-nociceptive signaling. These findings support a context-
539 dependent interaction between opioids and immune-derived signals [4,37].
540 Furthermore, our data reveal that this immune-neural disruption impairs cellular and network
541 homeostasis. Alterations in NeuN immunoreactivity likely reflect changes in neuronal functional state
542 and synaptic network integrity rather than overt neuronal loss, consistent with previous studies using
543 organotypic spinal cord cultures exposed to inflammatory stimuli [21]. Concurrently, changes in
544 GFAP expression and glial glutamate transporters EAAT1 and EAAT2 suggest a severe collapse of
545 astrocyte-mediated homeostatic mechanisms in response to mast cell mediators. Because astrocytes
546 are strictly required to clear extracellular glutamate, a reduction in EAAT2 expression leads to
547 extrasynaptic glutamate spillover, promoting excitotoxicity, and sustaining central sensitization and
548 chronic pain [38–40]. Together, these findings indicate that conditioned medium from activated mast
549 cells induces a neuroinflammatory and pro-nociceptive phenotype characterized by impaired neuron-
550 astrocyte homeostasis.
551 While morphine alone produced relatively modest changes in spinal cord slices, its presence markedly
552 exacerbated the effects of mast cell-conditioned medium. Morphine is increasingly recognized to
553 engage neuroimmune mechanisms beyond its direct neuronal actions, particularly through glial
554 activation and inflammatory signaling pathways [8,41,42]. In our model, the combination of
555 morphine and mast cell mediators resulted in enhanced inflammatory gene expression, further

dysregulation of astrocytic markers and altered glutamate transporter expression, indicating that morphine creates a permissive environment that amplifies immune-derived signaling.

Within this inflammatory and morphine-sensitized context, ultramicronized PEA exerted a definitive pro-homeostatic rescue via a sophisticated, dual-level mechanism. Upstream, PEA pre-treatment successfully reprogrammed the mast cell secretory activity. This observation is highly consistent with the autacoid local injury antagonism (ALIA) mechanism originally proposed by the Nobel laureate Rita Levi Montalcini [43], as well as with previous findings by our group [18]. Secretome analysis validated that PEA reduces the release of factors associated with mast cell activation, most notably the chemokine CCL2, a key regulator of neuroimmune communication in the spinal cord [44,45]. Downstream, direct application of PEA (50 nM) to the spinal slices efficiently intercepted neuroinflammatory cascades even after mast cell degranulation. Tissue-level PEA treatment strongly suppressed the transcription of IL-6, CCL2, and PTX3. These findings align with prior *in vivo* evidence demonstrating that PEA, reaching central nervous system structures [16], reduces inflammatory amplification in the injured spinal cord by limiting mast cell activation/infiltration and glial activation [46]. Furthermore, they parallel *ex vivo* data showing that PEA restrains spinal inflammatory enzymes and preserves neuronal readouts in multicellular spinal tissue preparations [47].

Functionally, ultramicronized PEA normalized CGRP release under inflammatory conditions without affecting baseline levels. This context-dependent effect is consistent with its ability to reduce the pathological neuroimmune and glial activation, and the production of inflammatory mediators in models of neuropathic and inflammatory pain, thereby attenuating central sensitization [13,28,48–50].

At the cellular level, PEA restored GFAP expression and normalized EAAT1 and EAAT2 profiles, suggesting the recovery of astrocyte-mediated glutamate homeostasis. As reported by Scuderi et al. (2012), PEA modulates astrocyte reactivity through PPAR-α-dependent mechanisms, as well as preserves the NeuN immunoreactivity supporting a stabilization of the neuroimmune environment

primarily acting on non-neuronal cells, such as mast cells and glia [13,51].

To better characterize the molecular landscape of spinal response to morphine, mast cell-derived factors and PEA, a quantitative proteomic analysis was performed, providing insight into coordinated changes across inflammatory, structural and homeostatic pathways.

Morphine alone induced a limited but biologically meaningful proteomic shift, characterized by upregulation of proteins involved in cytoskeletal regulation and immune signaling. One of them, PFN1 has been implicated in actin dynamics and inflammatory polarization of microglia, with PFN1 suppression shown to inhibit M1-like pro-inflammatory microglial states while promoting anti-inflammatory phenotypes [52,53]. Concurrently, morphine also increased RBM3 and DYNLRB1, which have been associated with cellular stress responses, neuronal survival and adaptive plasticity [54,55], suggesting the coexistence of early compensatory mechanisms that may nevertheless be insufficient to counterbalance inflammatory signaling.

Exposure of control slices to conditioned medium derived from activated mast cells produced a much broader proteomic remodeling, strongly skewed toward inflammatory and ECM-destabilizing pathways. Among the upregulated proteins, CTSD and BGN are of particular interest. CTSD has been shown to amplify neuroinflammation through activation of NF-κB signaling in microglia [56], while BGN functions as a damage-associated molecular pattern that activates TLR2 and TLR4 signaling, driving p38, ERK and NF-κB-dependent inflammatory cascades [57,58]. The concomitant downregulation of collagen type I chains in this condition suggests ECM remodeling toward a less stable microenvironment, consistent with recent evidence indicating that disruption of collagen-rich ECM contributes to CNS vulnerability and inflammatory amplification [59]. Together, these data support the view that mast cell mediators promote a feed-forward loop of neuroinflammation and matrix destabilization.

Strikingly, when spinal cord slices were exposed to conditioned medium from PEA-pretreated mast cells, this inflammatory signature was substantially reshaped. The proteomic profile was characterized by reduced expression of inflammatory ECM-associated mediators, such as BGN, and

608 increased expression of proteins associated with astrocytic regulation, including GFAP. This
609 observation is highly consistent with our previous findings in primary astrocyte cultures, where PEA-
610 conditioned mast cell media shifted astrocytes toward a less pro-inflammatory phenotype [18]. Given
611 the role of astrocytes in buffering inflammatory signals and maintaining tissue homeostasis, these
612 data suggest that ultramicronized PEA indirectly promotes a more regulated glial environment by
613 modifying mast cell outputs.
614 Co-exposure to morphine and conditioned medium from activated mast cells generated a highly
615 deleterious proteomic signature characterized by extensive downregulation of ECM components,
616 including collagen VI chains (COL6A1, 2, 3). Collagen VI is increasingly recognized as a
617 neuroprotective ECM component that regulates autophagy, oxidative stress and cell survival; its loss
618 severely enhances neuronal vulnerability and accelerates neurodegeneration [60,61]. This matrix
619 destabilization was coupled with the upregulation of BIN1, a known orchestrator of pro-inflammatory
620 microglial phenotype transitions [62], further supporting the idea that morphine amplifies mast cell-
621 driven neuroinflammation.
622 Notably, exposure of morphine-treated slices to conditioned media from PEA-treated mast cells
623 reshaped this microenvironment, inducing a robust upregulation of protective ECM components,
624 including a complete rescue of collagen VI and increased levels of anti-inflammatory proteins, like
625 LGALS1. LGALS1 has been shown to directly suppress TNF-α-induced oxidative stress, promote
626 protective M2-like microglial polarization, and actively inhibit IgE-mediated mast cell activation
627 [63,64], representing a powerful counter-regulatory safety mechanism. The concomitant
628 downregulation of SIRT2 is also highly relevant, as SIRT2 has been implicated in neurodegenerative
629 processes and its inhibition confers neuroprotection in several disease models [65]. Moreover, the
630 suppression of SIRT2 reduces FcεRI-dependent mast cell degranulation [66], providing a multi-level
631 dampening of mast cell-driven inflammatory loop.
632 When applied directly to nervous tissue, ultramicronized PEA also reduced the mast cell-driven
633 increase in CGRP release, restoring values toward baseline while leaving CGRP unchanged in control

slices. This pattern is compatible with a pro-homeostatic rather than suppressive profile and aligns with electrophysiological evidence that PEA can inhibit nociceptive-evoked responses of dorsal horn wide-dynamic-range neurons at the spinal level [67]. Finally, the accompanying changes in NeuN and GFAP immunoreactivity suggest that PEA mitigates mast cell-induced perturbations of neuronal marker expression and astrocytic activation, supporting the interpretation that PEA pro-homeostatically modulates the neuroimmune microenvironment of the dorsal horn during inflammatory challenge rather than acting as a generic neuronal suppressant [46].

In conclusion, our findings suggest that ultramicronized PEA may play a vital dual role within the spinal neuroimmune interface. By acting both upstream to blunt the primary mast cell inflammatory output and downstream to protect spinal dorsal horn architectures from ongoing inflammatory challenges, PEA appears to preserve the physiological crosstalk within the neuron-glia-matrix network. This integrated mechanism provides a solid translational rationale for incorporating ultramicronized PEA as a potential adjunctive strategy to counteract neuroimmune maladaptation and matrix destabilization. Beyond conceivably sustaining target drug efficacy, such as mitigating morphine-induced dysregulation, this dual-level control offers a promising approach to modulate the development of central sensitization, thereby opening new clinical avenues for the management of chronic and neuroinflammatory pain states.

Acknowledgments: Not applicable

Conflict of interest

The authors declare that they have no known competing financial interests or personal relationships that could have appeared to influence the work reported in this paper. Carla Ghelardini and Lorenzo Di Cesare Mannelli received a grant from Epitech (Padua, Italy).

Author Contributions

AT: data curation, formal analysis, methodology, writing – original draft. MGC: data curation, formal analysis, methodology, writing – original draft. LM: conceptualization, visualization, writing and editing; EL: visualization, writing and editing; FM: formal analysis and methodology; DV: formal analysis and methodology; GA: formal analysis and methodology. AD: formal analysis, methodology and writing. TM: formal analysis, methodology, writing and editing. CG: conceptualization, funding acquisition, supervision, writing and editing. LDCM: conceptualization, funding acquisition, supervision, writing and editing.

Co-author details

Maria Giovanna Cataldi: mariagiovanna.cataldi@unifi.it, ORCID: 0009-0003-3016-5834

Laura Micheli: laura.micheli@unifi.it, ORCID: 0000-0002-6806-3222

Elena Lucarini: elena.lucarini@unifi.it, ORCID: 0000-0002-3459-2660

Francesco Margiotta: f.margiotta@ebris.eu, francesco.margiotta@unifi.it, ORCID: 0000-0002-6608-5399

Daniel Venturi: daniel.venturi@ndcn.ox.ac.uk, daniel.venturi1@unifi.it, ORCID: 0009-0006-3933-0236

Gilda Aiello: gilda.aiello@uniroma5.it, ORCID: 0000-0003-4327-0521

Alfonsina D'Amato: alfonsina.damato@unimi.it, ORCID: 0000-0002-8147-7235

Tommaso Mello: tommaso.mello@unifi.it, ORCID: 0000-0002-6192-6902

Carla Ghelardini: carla.ghelardini@unifi.it, ORCID: 0000-0001-9856-8144

Lorenzo Di Cesare Mannelli: lorenzo.mannelli@unifi.it, ORCID: 0000-0001-8374-4432

Availability of data and material

The data that support the findings of this study are available from the corresponding author on reasonable request.

Funding

This work was supported by the European Union - NextGenerationEU - National Recovery and Resilience Plan, Mission 4 Component 2 - Investment 1.4 – Strengthening research facilities and creation of "Campioni Nazionali di R&S" on Key Enabling Technologies - National Center for Gene Therapy and Drugs based on RNA Technology - CN00000041 - CUP B13C22001010001; by National Recovery and Resilience Plan, project MNESYS (PE00000006) – A Multiscale integrated approach to the study of the nervous system in health and disease (DN. 1553 11.10.2022) and the Italian Ministry of University and Research (MIUR).

Declaration of AI-assisted language editing

During the preparation of this manuscript, the author used an artificial-intelligence-based tool solely for the purpose of editing the English language (grammar, style, clarity). No generative AI was used to create, analyze or interpret the scientific content of the work. All final wording, arguments, data interpretation and conclusions remain entirely the responsibility of the authors.

References

1. Raja SN, Carr DB, Cohen M, Finnerup NB, Flor H, Gibson S, et al. The revised International Association for the Study of Pain definition of pain: concepts, challenges, and compromises. Pain. 2020;161:1976–82. https://doi.org/10.1097/j.pain.0000000000001939

2. Basbaum AI, Bautista DM, Scherrer G, Julius D. Cellular and molecular mechanisms of pain. Cell. 2009;139:267–84. https://doi.org/10.1016/j.cell.2009.09.028

3. Woolf CJ. Central sensitization: implications for the diagnosis and treatment of pain. Pain. 2011;152:S2–15. https://doi.org/10.1016/j.pain.2010.09.030

4. Grace PM, Hutchinson MR, Maier SF, Watkins LR. Pathological pain and the neuroimmune

710 interface. Nat Rev Immunol. 2014;14:217–31. https://doi.org/10.1038/nri3621

711 5. Lambert DG. Opioids and opioid receptors; understanding pharmacological mechanisms as a key
712 to therapeutic advances and mitigation of the misuse crisis. BJA Open. 2023;6:100141.
713 https://doi.org/10.1016/j.bjao.2023.100141

714 6. Roeckel L-A, Utard V, Reiss D, Mouheiche J, Maurin H, Robé A, et al. Morphine-induced
715 hyperalgesia involves mu opioid receptors and the metabolite morphine-3-glucuronide. Sci Rep.
716 2017;7:10406. https://doi.org/10.1038/s41598-017-11120-4

717 7. Zhou J, Ma R, Jin Y, Fang J, Du J, Shao X, et al. Molecular mechanisms of opioid tolerance:
718 From opioid receptors to inflammatory mediators (Review). Exp Ther Med. 2021;22:1004.
719 https://doi.org/10.3892/etm.2021.10437

720 8. Hutchinson MR, Bland ST, Johnson KW, Rice KC, Maier SF, Watkins LR. Opioid-induced glial
721 activation: mechanisms of activation and implications for opioid analgesia, dependence, and
722 reward. ScientificWorldJournal. 2007;7:98–111. https://doi.org/10.1100/tsw.2007.230

723 9. Mittal A, Sagi V, Gupta M, Gupta K. Mast Cell Neural Interactions in Health and Disease. Front
724 Cell Neurosci. 2019;13:110. https://doi.org/10.3389/fncel.2019.00110

725 10. Polyzoidis S, Koletsa T, Panagiotidou S, Ashkan K, Theoharides TC. Mast cells in
726 meningiomas and brain inflammation. J Neuroinflammation. 2015;12:170.
727 https://doi.org/10.1186/s12974-015-0388-3

728 11. Levy D. Migraine pain, meningeal inflammation, and mast cells. Curr Pain Headache Rep.
729 2009;13:237–40. https://doi.org/10.1007/s11916-009-0040-y

730 12. Varrassi G, Fusco M, Skaper SD, Battelli D, Zis P, Coaccioli S, et al. A Pharmacological
731 Rationale to Reduce the Incidence of Opioid Induced Tolerance and Hyperalgesia: A Review. Pain

732 Ther. 2018;7:59–75. https://doi.org/10.1007/s40122-018-0094-9

733 13. Petrosino S, Di Marzo V. The pharmacology of palmitoylethanolamide and first data on the
734 therapeutic efficacy of some of its new formulations. Br J Pharmacol. 2017;174:1349–65.
735 https://doi.org/10.1111/bph.13580

736 14. Impellizzeri D, Bruschetta G, Cordaro M, Crupi R, Siracusa R, Esposito E, et al.
737 Micronized/ultramicronized palmitoylethanolamide displays superior oral efficacy compared to
738 nonmicronized palmitoylethanolamide in a rat model of inflammatory pain. J Neuroinflammation.
739 2014;11:136. https://doi.org/10.1186/s12974-014-0136-0

740 15. Nobili S, Micheli L, Lucarini E, Toti A, Ghelardini C, Di Cesare Mannelli L. Ultramicronized
741 N-palmitoylethanolamine associated with analgesics: Effects against persistent pain. Pharmacol
742 Ther. 2024;258:108649. https://doi.org/10.1016/j.pharmthera.2024.108649

743 16. Petrosino S, Cordaro M, Verde R, Schiano Moriello A, Marcolongo G, Schievano C, et al. Oral
744 Ultramicronized Palmitoylethanolamide: Plasma and Tissue Levels and Spinal Anti-hyperalgesic
745 Effect. Front Pharmacol. 2018;9:249. https://doi.org/10.3389/fphar.2018.00249

746 17. Di Cesare Mannelli L, Micheli L, Lucarini E, Ghelardini C. Ultramicronized N-
747 Palmitoylethanolamine Supplementation for Long-Lasting, Low-Dosed Morphine Antinociception.
748 Front Pharmacol. 2018;9:473. https://doi.org/10.3389/fphar.2018.00473

749 18. Toti A, Micheli L, Lucarini E, Ferrara V, Ciampi C, Margiotta F, et al. Ultramicronized N-
750 Palmitoylethanolamine Regulates Mast Cell-Astrocyte Crosstalk: A New Potential Mechanism
751 Underlying the Inhibition of Morphine Tolerance. Biomolecules. 2023;13:233.
752 https://doi.org/10.3390/biom13020233

753 19. Micheli L, Lucarini E, Nobili S, Bartolucci G, Pallecchi M, Toti A, et al. Ultramicronized N-
754 palmitoylethanolamine Contributes to Morphine Efficacy Against Neuropathic Pain: Implication of

755 Mast Cells and Glia. Curr Neuropharmacol. 2024;22:88–106.
756 https://doi.org/10.2174/1570159X21666221128091453

757 20. Humpel C. Organotypic brain slice cultures: A review. Neuroscience. 2015;305:86–98.
758 https://doi.org/10.1016/j.neuroscience.2015.07.086

759 21. Ravikumar M, Jain S, Miller RH, Capadona JR, Selkirk SM. An organotypic spinal cord slice
760 culture model to quantify neurodegeneration. J Neurosci Methods. 2012;211:280–8.
761 https://doi.org/10.1016/j.jneumeth.2012.09.004

762 22. McGrath JC, Lilley E. Implementing guidelines on reporting research using animals (ARRIVE
763 etc.): new requirements for publication in BJP. Br J Pharmacol. 2015;172:3189–93.
764 https://doi.org/10.1111/bph.12955

765 23. Toti A, Lucarini E, Ferrara V, Parisio C, Ciampi C, Gerace E, et al. The dual role of VEGF-A in
766 a complex in vitro model of oxaliplatin-induced neurotoxicity: Pain-related and neuroprotective
767 effects. Neurotherapeutics. 2025;22:e00532. https://doi.org/10.1016/j.neurot.2025.e00532

768 24. D'Amato A, Di Cesare Mannelli L, Lucarini E, Man AL, Le Gall G, Branca JJV, et al. Faecal
769 microbiota transplant from aged donor mice affects spatial learning and memory via modulating
770 hippocampal synaptic plasticity- and neurotransmission-related proteins in young recipients.
771 Microbiome. 2020;8:140. https://doi.org/10.1186/s40168-020-00914-w

772 25. Radrezza S, Carini M, Baron G, Aldini G, Negre-Salvayre A, D'Amato A. Study of Carnosine's
773 effect on nude mice skin to prevent UV-A damage. Free Radic Biol Med. 2021;173:97–103.
774 https://doi.org/10.1016/j.freeradbiomed.2021.07.010

775 26. Cox J, Hein MY, Luber CA, Paron I, Nagaraj N, Mann M. Accurate proteome-wide label-free
776 quantification by delayed normalization and maximal peptide ratio extraction, termed MaxLFQ.
777 Mol Cell Proteomics. 2014;13:2513–26. https://doi.org/10.1074/mcp.M113.031591

778 27. Theoharides TC, Tsilioni I, Ren H. Recent advances in our understanding of mast cell activation
779 – or should it be mast cell mediator disorders? Expert Rev Clin Immunol. 2019;15:639–56.
780 https://doi.org/10.1080/1744666X.2019.1596800

781 28. Skaper SD, Facci L, Fusco M, Della Valle MF, Zusso M, Costa B, et al. Palmitoylethanolamide,
782 a naturally occurring disease-modifying agent in neuropathic pain. Inflammopharmacology.
783 2014;22:79–94. https://doi.org/10.1007/s10787-013-0191-7

784 29. Levy D, Burstein R, Kainz V, Jakubowski M, Strassman AM. Mast cell degranulation activates
785 a pain pathway underlying migraine headache. Pain. 2007;130:166–76.
786 https://doi.org/10.1016/j.pain.2007.03.012

787 30. Kawasaki Y, Zhang L, Cheng J-K, Ji R-R. Cytokine mechanisms of central sensitization:
788 distinct and overlapping role of interleukin-1beta, interleukin-6, and tumor necrosis factor-alpha in
789 regulating synaptic and neuronal activity in the superficial spinal cord. J Neurosci. 2008;28:5189–
790 94. https://doi.org/10.1523/JNEUROSCI.3338-07.2008

791 31. White FA, Bhangoo SK, Miller RJ. Chemokines: integrators of pain and inflammation. Nat Rev
792 Drug Discov. 2005;4:834–44. https://doi.org/10.1038/nrd1852

793 32. Fan M, Liang Z, Shen J, Yang H, Zhao L, Li M, et al. The function of chemokine-driven glial-
794 neuronal interaction in chronic pain. Front Neurosci. 2026;20:1830053.
795 https://doi.org/10.3389/fnins.2026.1830053

796 33. Russell FA, King R, Smillie S-J, Kodji X, Brain SD. Calcitonin gene-related peptide:
797 physiology and pathophysiology. Physiol Rev. 2014;94:1099–142.
798 https://doi.org/10.1152/physrev.00034.2013

799 34. Iyengar S, Ossipov MH, Johnson KW. The role of calcitonin gene-related peptide in peripheral
800 and central pain mechanisms including migraine. Pain. 2017;158:543–59.

https://doi.org/10.1097/j.pain.0000000000000831

35. Wang Z, Ma W, Chabot J-G, Quirion R. Calcitonin gene-related peptide as a regulator of neuronal CaMKII-CREB, microglial p38-NFκB and astroglial ERK-Stat1/3 cascades mediating the development of tolerance to morphine-induced analgesia. Pain. 2010;151:194–205. https://doi.org/10.1016/j.pain.2010.07.006

36. Ji R-R, Nackley A, Huh Y, Terrando N, Maixner W. Neuroinflammation and Central Sensitization in Chronic and Widespread Pain. Anesthesiology. 2018;129:343–66. https://doi.org/10.1097/ALN.0000000000002130

37. Bannister K, Dickenson AH. What the brain tells the spinal cord. Pain. 2016;157:2148–51. https://doi.org/10.1097/j.pain.0000000000000568

38. Di Cesare Mannelli L, Pacini A, Micheli L, Tani A, Zanardelli M, Ghelardini C. Glial role in oxaliplatin-induced neuropathic pain. Exp Neurol. 2014;261:22–33. https://doi.org/10.1016/j.expneurol.2014.06.016

39. Nie H, Weng H-R. Impaired glial glutamate uptake induces extrasynaptic glutamate spillover in the spinal sensory synapses of neuropathic rats. J Neurophysiol. 2010;103:2570–80. https://doi.org/10.1152/jn.00013.2010

40. Popiolek-Barczyk K, Mika J. Targeting the Microglial Signaling Pathways: New Insights in the Modulation of Neuropathic Pain. Curr Med Chem. 2016;23:2908–28. https://doi.org/10.2174/0929867323666160607120124

41. Di Cesare Mannelli L, Corti F, Micheli L, Zanardelli M, Ghelardini C. Delay of morphine tolerance by palmitoylethanolamide. Biomed Res Int. 2015;2015:894732. https://doi.org/10.1155/2015/894732

823 42. Yang Y, Sun Y, Hu R, Yan J, Wang Z, Li W, et al. Morphine promotes microglial activation by
824 upregulating the EGFR/ERK signaling pathway. PLoS One. 2021;16:e0256870.
825 https://doi.org/10.1371/journal.pone.0256870

826 43. Aloe L, Leon A, Levi-Montalcini R. A proposed autacoid mechanism controlling mastocyte
827 behaviour. Agents Actions. 1993;39 Spec No:C145-147. https://doi.org/10.1007/BF01972748

828 44. Abbadie C, Lindia JA, Cumiskey AM, Peterson LB, Mudgett JS, Bayne EK, et al. Impaired
829 neuropathic pain responses in mice lacking the chemokine receptor CCR2. Proc Natl Acad Sci U S
830 A. 2003;100:7947–52. https://doi.org/10.1073/pnas.1331358100

831 45. Zhang J, Shi XQ, Echeverry S, Mogil JS, De Koninck Y, Rivest S. Expression of CCR2 in both
832 resident and bone marrow-derived microglia plays a critical role in neuropathic pain. J Neurosci.
833 2007;27:12396–406. https://doi.org/10.1523/JNEUROSCI.3016-07.2007

834 46. Esposito E, Paterniti I, Mazzon E, Genovese T, Di Paola R, Galuppo M, et al. Effects of
835 palmitoylethanolamide on release of mast cell peptidases and neurotrophic factors after spinal cord
836 injury. Brain Behav Immun. 2011;25:1099–112. https://doi.org/10.1016/j.bbi.2011.02.006

837 47. Paterniti I, Impellizzeri D, Di Paola R, Navarra M, Cuzzocrea S, Esposito E. A new co-
838 ultramicronized composite including palmitoylethanolamide and luteolin to prevent
839 neuroinflammation in spinal cord injury. J Neuroinflammation. 2013;10:91.
840 https://doi.org/10.1186/1742-2094-10-91

841 48. Di Cesare Mannelli L, D'Agostino G, Pacini A, Russo R, Zanardelli M, Ghelardini C, et al.
842 Palmitoylethanolamide Is a Disease-Modifying Agent in Peripheral Neuropathy: Pain Relief and
843 Neuroprotection Share a PPAR-Alpha-Mediated Mechanism. Mediators Inflamm.
844 2013;2013:328797. https://doi.org/10.1155/2013/328797

845 49. Scuderi C, Stecca C, Valenza M, Ratano P, Bronzuoli MR, Bartoli S, et al.

846 Palmitoylethanolamide controls reactive gliosis and exerts neuroprotective functions in a rat model
847 of Alzheimer's disease. Cell Death Dis. 2014;5:e1419. https://doi.org/10.1038/cddis.2014.376

848 50. Di Cesare Mannelli L, Pacini A, Corti F, Boccella S, Luongo L, Esposito E, et al.
849 Antineuropathic profile of N-palmitoylethanolamine in a rat model of oxaliplatin-induced
850 neurotoxicity. PLoS One. 2015;10:e0128080. https://doi.org/10.1371/journal.pone.0128080

851 51. Scuderi C, Valenza M, Stecca C, Esposito G, Carratù MR, Steardo L. Palmitoylethanolamide
852 exerts neuroprotective effects in mixed neuroglial cultures and organotypic hippocampal slices via
853 peroxisome proliferator-activated receptor-α. J Neuroinflammation. 2012;9:49.
854 https://doi.org/10.1186/1742-2094-9-49

855 52. Lu E, Wang Q, Li S, Chen C, Wu W, Xu YXZ, et al. Profilin 1 knockdown prevents ischemic
856 brain damage by promoting M2 microglial polarization associated with the RhoA/ROCK pathway.
857 J Neurosci Res. 2020;98:1198–212. https://doi.org/10.1002/jnr.24607

858 53. Pereira GRC, Tellini GHAS, De Mesquita JF. In silico analysis of PFN1 related to amyotrophic
859 lateral sclerosis. PLoS One. 2019;14:e0215723. https://doi.org/10.1371/journal.pone.0215723

860 54. Pilotte J, Kiosses W, Chan SW, Makarenkova HP, Dupont-Versteegden E, Vanderklish PW.
861 Morphoregulatory functions of the RNA-binding motif protein 3 in cell spreading, polarity and
862 migration. Sci Rep. 2018;8:7367. https://doi.org/10.1038/s41598-018-25668-2

863 55. Terenzio M, Di Pizio A, Rishal I, Marvaldi L, Di Matteo P, Kawaguchi R, et al. DYNLRB1 is
864 essential for dynein mediated transport and neuronal survival. Neurobiol Dis. 2020;140:104816.
865 https://doi.org/10.1016/j.nbd.2020.104816

866 56. Gan P, Xia Q, Hang G, Zhou Y, Qian X, Wang X, et al. Knockdown of cathepsin D protects
867 dopaminergic neurons against neuroinflammation-mediated neurotoxicity through inhibition of NF-
868 κB signalling pathway in Parkinson's disease model. Clin Exp Pharmacol Physiol. 2019;46:337–49.

869 https://doi.org/10.1111/1440-1681.13052

870 57. Schaefer L, Babelova A, Kiss E, Hausser H-J, Baliova M, Krzyzankova M, et al. The matrix
871 component biglycan is proinflammatory and signals through Toll-like receptors 4 and 2 in
872 macrophages. J Clin Invest. 2005;115:2223–33. https://doi.org/10.1172/JCI23755

873 58. Roedig H, Nastase MV, Wygrecka M, Schaefer L. Breaking down chronic inflammatory
874 diseases: the role of biglycan in promoting a switch between inflammation and autophagy. FEBS J.
875 2019;286:2965–79. https://doi.org/10.1111/febs.14791

876 59. Wareham LK, Baratta RO, Del Buono BJ, Schlumpf E, Calkins DJ. Collagen in the central
877 nervous system: contributions to neurodegeneration and promise as a therapeutic target. Mol
878 Neurodegener. 2024;19:11. https://doi.org/10.1186/s13024-024-00704-0

879 60. Chen P, Cescon M, Megighian A, Bonaldo P. Collagen VI regulates peripheral nerve
880 myelination and function. FASEB J. 2014;28:1145–56. https://doi.org/10.1096/fj.13-239533

881 61. Cescon M, Chen P, Castagnaro S, Gregorio I, Bonaldo P. Lack of collagen VI promotes
882 neurodegeneration by impairing autophagy and inducing apoptosis during aging. Aging (Albany
883 NY). 2016;8:1083–101. https://doi.org/10.18632/aging.100924

884 62. Sudwarts A, Ramesha S, Gao T, Ponnusamy M, Wang S, Hansen M, et al. BIN1 is a key
885 regulator of proinflammatory and neurodegeneration-related activation in microglia. Mol
886 Neurodegener. 2022;17:33. https://doi.org/10.1186/s13024-022-00535-x

887 63. Aalinkeel R, Mangum CS, Abou-Jaoude E, Reynolds JL, Liu M, Sundquist K, et al. Galectin-1
888 Reduces Neuroinflammation via Modulation of Nitric Oxide-Arginase Signaling in HIV-1
889 Transfected Microglia: a Gold Nanoparticle-Galectin-1 “Nanoplex” a Possible Neurotherapeutic? J
890 Neuroimmune Pharmacol. 2017;12:133–51. https://doi.org/10.1007/s11481-016-9723-4

64. Yang L-T, Shu Q, Luo X-Q, Liu Z-Q, Qiu S-Q, Liu J-Q, et al. Long-term effects: Galectin-1 and specific immunotherapy for allergic responses in the intestine. Allergy. 2018;73:106–14. https://doi.org/10.1111/all.13256

65. Donmez G, Outeiro TF. SIRT1 and SIRT2: emerging targets in neurodegeneration. EMBO Mol Med. 2013;5:344–52. https://doi.org/10.1002/emmm.201302451

66. Kim Y-Y, Hur G, Lee SW, Lee S-J, Lee S, Kim S-H, et al. AGK2 ameliorates mast cell-mediated allergic airway inflammation and fibrosis by inhibiting FcεRI/TGF-β signaling pathway. Pharmacol Res. 2020;159:105027. https://doi.org/10.1016/j.phrs.2020.105027

67. González-Hernández A, Martínez-Lorenzana G, Rodríguez-Jiménez J, Rojas-Piloni G, Condés-Lara M. Intracisternal injection of palmitoylethanolamide inhibits the peripheral nociceptive evoked responses of dorsal horn wide dynamic range neurons. J Neural Transm (Vienna). Vienna, Austria : 1996; 2015;122:369–74. https://doi.org/10.1007/s00702-014-1255-6

Notes

The images shown in the figures panels to illustrate immunofluorescence data were processed using the Thunder algorithm (Leica Software) to reduce background noise. Entire Thunder-processed images were subsequently adjusted for contrast and brightness to improve presentation clarity.

Supplementary Files

This is a list of supplementary files associated with this preprint. Click to download.

- SupplementaryMaterial.docx